Communication

Non-Destructive Diagnosis on the Masaccio Frescoes at the Brancacci Chapel, Church of Santa Maria del Carmine (Florence)

Giovanni Leucci [1,*] , **Lara De Giorgi** [1] , **Ivan Ferrari** [1] , **Francesco Giuri** [1] , **Lucrezia Longhitano** [2] , **Alberto Felici** [3] **and Cristiano Riminesi** [4]

1   Institute of Heritage Sciences, National Research Council, 73100 Lecce, Italy
2   Department of Humanities, University of Catania, 95124 Catania, Italy
3   SABAP di Firenze, 50125 Firenze, Italy
4   Institute of Heritage Sciences, National Research Council, 50019 Sesto Fiorentino, Italy
*   Correspondence: giovanni.leucci@cnr.it

Abstract: The Basilica of Santa Maria del Carmine in Florence, in the Oltrarno area, was built in 1268 (pre-Renaissance low medieval context) and consecrated in 1422. Following a devastating fire in the interior of the original church, in 1771, very little remained. Among the parts that were saved were the Corsini and Brancacci chapels. The architect Giuseppe Ruggeri was responsible for the reconstruction of the church, which was completed in 1782 (with the exception of the gabled façade which remained unfinished, as can still be seen today). Geophysical investigations were undertaken into the Brancacci chapel in order to have information on the structure of the wall that contains wall paintings by Masaccio, Masolino, and Filippino Lippi, to understand the stratigraphy of the mortars, and to formulate some hypotheses on the causes of their detachment. The results are interesting.

Keywords: GPR; Masaccio frescoes; diagnosis; Florence

1. Introduction

Inside the church of Santa Maria del Carmine, in Florence, is the Brancacci Chapel (Figure 1), located to the southwest, to the left of the transept. It was miraculously saved from the devastating fire of 1771, together with the Corsini Chapel (opposite side of the transept). It belonged to the Florentine Brancacci family (to which it owes its name) from the second half of the 1300s until the 1780s, then passed to the Riccardi family. Felice Brancacci, who was the patron of the chapel from 1422 until about 1436, and a leading exponent of the Florentine nobility, following his return from the role of ambassador to Cairo, commissioned the pictures that characterize the chapel and make it famous.

The paintings were the work of the important Renaissance artists Masaccio (Tommaso di Mone Cassai; Castel San Giovanni, 1401-Rome, 1428) and Masolino da Panicale (Tommaso di Cristoforo Fini; Panicale, 1383-Florence, 1440), completed by Filippino Lippi (Prato, 1457-Florence, 1504). The decorative were painted between 1422 and 1475.

The cycle represented concerns the stories of the life of Saint Peter, drawing the events from the Gospels, the Acts of the Apostles, and the Golden Legend, as well as two moments taken from Genesis. The importance and fame of the Brancacci Chapel are largely due to the presence of the works by Masaccio who, although a young painter, who died at the age of twenty-seven, was the architect of a new vision in the field of painting at the beginning of the fifteenth century (Figure 2).

On the walls of the Brancacci Chapel, Masaccio collaborated on an equal footing with Masolino, an older painter than himself, starting from the end of 1424. The cycle remained unfinished and was completed fifty years later by Filippino Lippi, who also had the task of compensating some faces that had been erased to obscure the memory of Felice Brancacci's client. In fact, Felice Brancacci was declared an enemy of the Republic, and exiled. For a long time, due to the conditions of the pictorial surface, blackened by the smoke of the

candles, it was difficult to attribute the scenes to each of the two artists. With the important twentieth-century restoration, which made the situation more clear, it was possible to make the attributions more solid. To support the thesis that Masolino and Masaccio worked simultaneously in this chapel, there is the extraordinary perspective unity of the scenes in this cycle: not only does each panel have its own vanishing point, and it is towards this that all the lines of depth converge, but the individual vanishing points of the scenes on the opposite walls fit together perfectly. In other words, the perspective layout of the two scenes viewed from the front, if reversed, can be superimposed. On the back wall, on the other hand, the vanishing point is external to the scenes, and matches the geometric centre of the wall.

Figure 1. The Brancacci chapel.
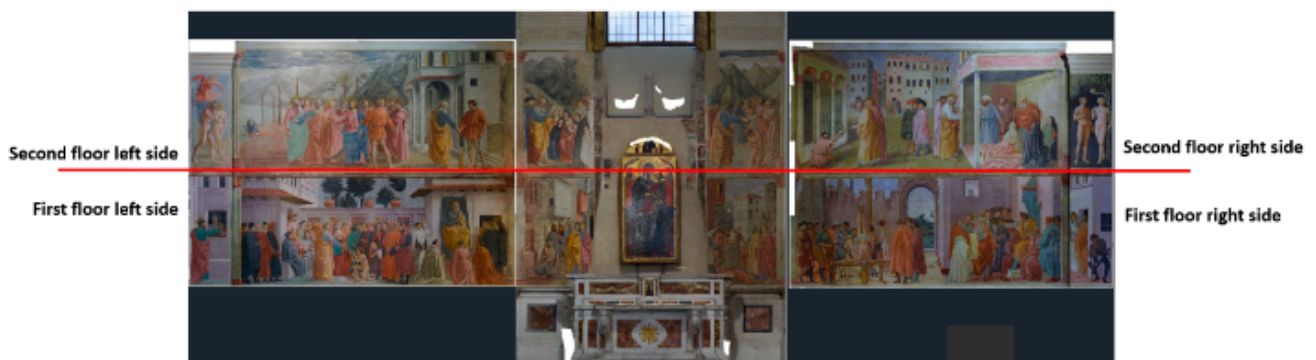
Figure 2. The wall paintings with indication of the areas investigated with the GPR.

Geophysical survey methods are non-destructive and can provide important information on the state of conservation of the built cultural heritage. During the restoration phase, they can help to determine the most appropriate intervention strategies. Ground penetrating radar (GPR) is the geophysical methodology that has been increasingly used in recent years, thanks to its ability to provide high-resolution data with relatively short acquisition times [1,2]. For example, it helps to identify voids or cavities, defects such as fractures, lesions, masonry structures, etc. [1–5]. The GPR methodology has also been successfully used in the study of the internal structure of wooden beams and columns [3]. For the study of the state of conservation of the frescoes, GPR may be able to provide information on the structural conditions of the walls that support the paintings [5–8]. Some interesting applications are shown in [5]. The purpose of this research was to estimate the state of conservation of the wall structure containing the frescoes by Masaccio and Masolino, and the state of conservation of the paintings, by means of 3D analysis. The results obtained are useful for determining the degree of lack of adhesion of the layers underlying the painting, in order to plan the restoration in situ.

2. Materials and Methods

The GPR methodology is related to the study of the propagation of electromagnetic (EM) waves. EM waves are transmitted by an emitting antenna through the medium to be studied [1–3]. They propagate, and are subsequently reflected if they encounter a discontinuity with different electromagnetic characteristics (for example voids) from those of the medium in which they are propagating. The reflected EM waves are received by a receiving antenna and the result can be seen in real-time on a computer screen. The frequencies generally used range from 10 MHz to about 2600 MHz. The physical parameters that characterize the propagation of EM waves are relative dielectric permittivity, electrical conductivity, and magnetic permittivity.

Another important physical parameter is the velocity of propagation of the EM waves. For the GPR frequency range, the velocity is mainly linked to the relative dielectric permittivity of the medium being investigated, and also depends on the volumetric water content. In fact, the higher the volumetric water content, the lower the velocity of propagation of the EM waves [1–3]. Therefore, from the estimate of the velocity of propagation of the EM waves, it is possible to estimate the relative dielectric permittivity (ε_r), and subsequently the volumetric water content (w). The volumetric water content (w) assumes relevant importance in this study of the state of conservation of the frescoes [1]. In this case study, the GPR survey was performed using an RIS MF Hi-Mod ground penetrating radar (IDS), with antennas with nominal frequencies of 900 MHz and 2000 MHz.

The chosen frequencies allow for a high vertical and horizontal resolution (2000 MHz), and a good penetration of the EM wave (900 MHz) [1–3].

In the GPR data acquisition, special precautions were taken to prevent the antenna from crawling, and consequently ruining the frescoes. The antenna was kept at a distance of about 1 cm from the frescoes' surface (Figure 3). The GPR data were acquired within a regular grid, with a step-size of 0.05 m. There were 512 samples per trace, with a trace interval of 0.002 m. Furthermore, a time window of 10 ns was set for the 2000 MHz antenna, while the time window was 70 ns for the 900 MHz antenna. The type of acquisition made it possible to carry out a 3D analysis of the results through the construction of time slices and isosurfaces of the EM amplitude [1–4].

Figure 3. Photos from the GPR data acquisition phase.

3. Results

The most interesting results related to the two antennas will be presented here.

3.1. 900 MHz Antenna Data Analysis

The GPR data were processed in a first phase using the reflexW software [9] using: (i) Time–zero correction, to compensate for the distance antenna–wall; (ii) manual gain, to adjust the acquisition gain function and enhance the visibility of deeper anomalies; (iii) background removal, to attenuate the horizontal banding in the deeper part of the sections (ringing), performed by subtracting in different time ranges a local average noise trace estimated from suitably selected time–distance windows with low signal content (this local subtraction procedure was necessary to avoid artefacts created by the classic subtraction of a global average trace estimated from the entire section, due to the presence of zones with a very strong signal); (iv) bandpass frequency filtering, in order to eliminate the components of low and high frequency noise (50–1500 MHz); (v) estimation of the average electromagnetic wave velocity by hyperbola fitting; (vi) Kirchhoff migration, using the 2D velocity distribution [1–4].

Some processed GPR profiles related to the second-floor right side, and to the 900 MHz antenna, are shown in Figure 4. Here, data analysis highlighted:
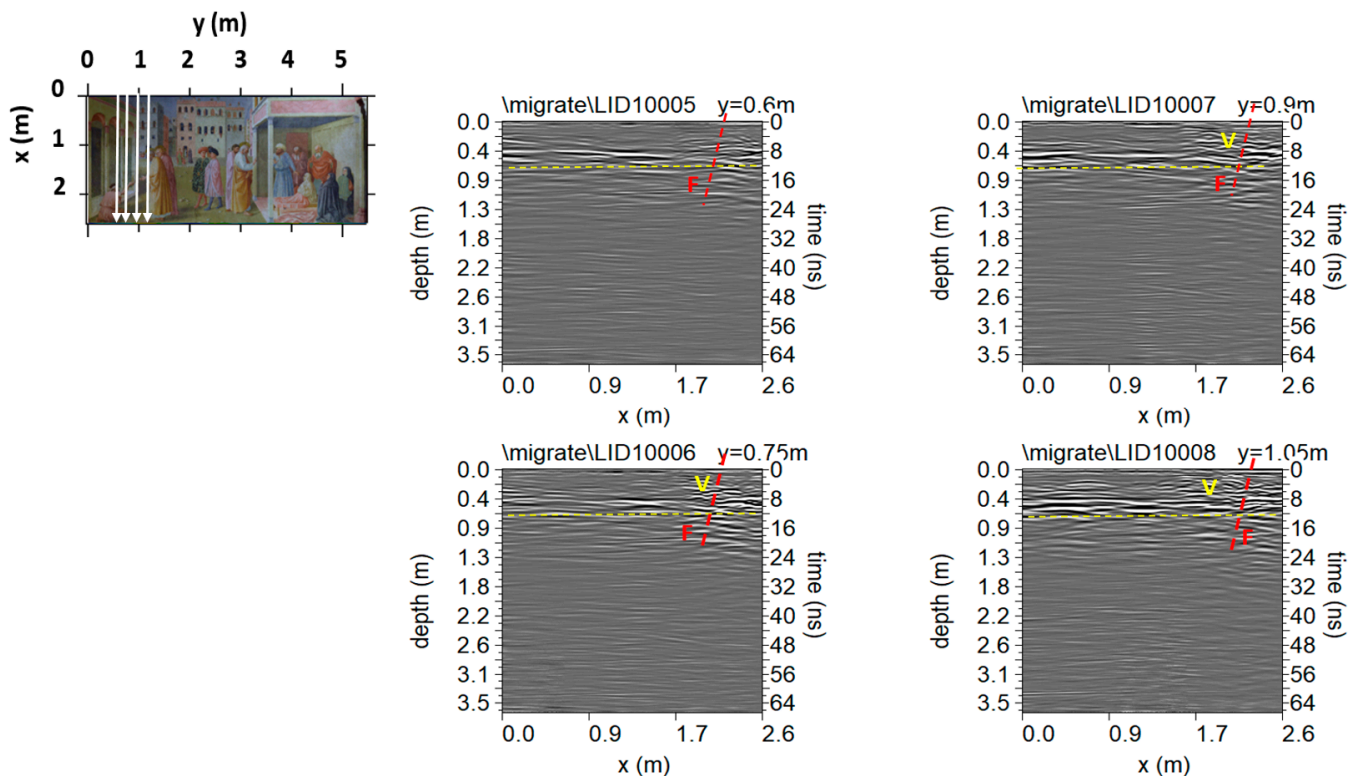
Figure 4. Second floor right side, large fresco, 900 MHz antenna: processed radar vertical sections related to profiles 5–8. The dotted yellow line represents the outer limit of the masonry. F: fracture; V: empty.

- A good penetration of the signal, which allows delimiting of the thickness of the masonry (dashed yellow line); this thickness is estimated to be between about 0.55 m and 0.6 m (with an average velocity of propagation of the electromagnetic wave equal to 0.11 m/ns);
- A series of reflection events, indicated by the dotted red lines and denominated F, which can probably be interpreted as relating to the presence of fractures inside the masonry; in particular, in correspondence with the cracks, a probable event of settling of the masonry is highlighted. This could be linked to a series of water infiltrations in the foundations due to heavy rains;

- A series of reflection events (V), which could be interpreted as being due to the probable presence of small voids. In fact, here, a change in the polarity of the reflected electromagnetic signal was noticed [1–3].

At the point indicated with V in Figure 4, it is possible to see a bulge of the lower part of the fresco (Figure 5).
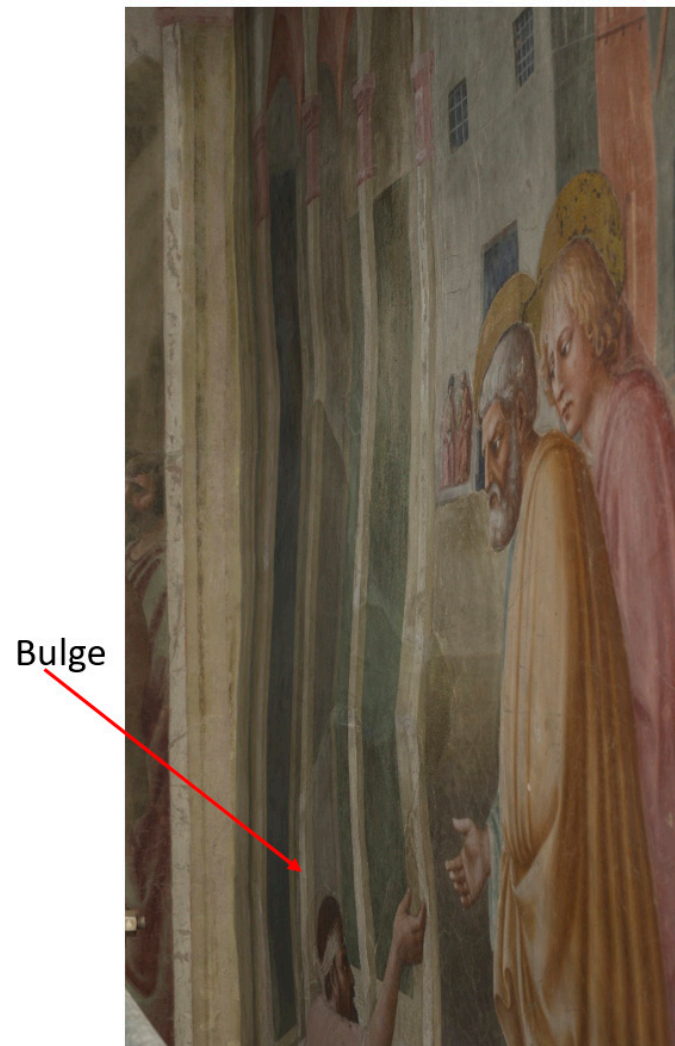
Figure 5. Bulge present on the fresco.

The method of acquiring the data, within a regular grid with a pitch equal to 0.05 m, has allowed the creation of a 3D visualization of the results, using time-slices and envelope isosurfaces of the electromagnetic waves. These are maps on which the reflection amplitudes have been projected at a specified time (or depth), with a selected time interval [1–4]. Moreover, the envelope of highest amplitudes were rendered into an isosurface [1–3]. Three-dimensional amplitude isosurface rendering displays amplitudes of equal value in the GPR study volume. Shading is usually used to illuminate these surfaces, giving the appearance of real anomalies. Clearly, the choice of the threshold is the most delicate aspect, and it is linked to the experience of those who process the data [1–3].

In this case, time slices were created using the GPR-slice software [10], with a time interval of 3.4 ns. Figure 6a shows the most significant time slices.

In this last figure, it is possible to notice the main anomalies (F and V) at various depths. Figure 6b shows a 3D view that allows one to follow the development of the F and V anomalies.
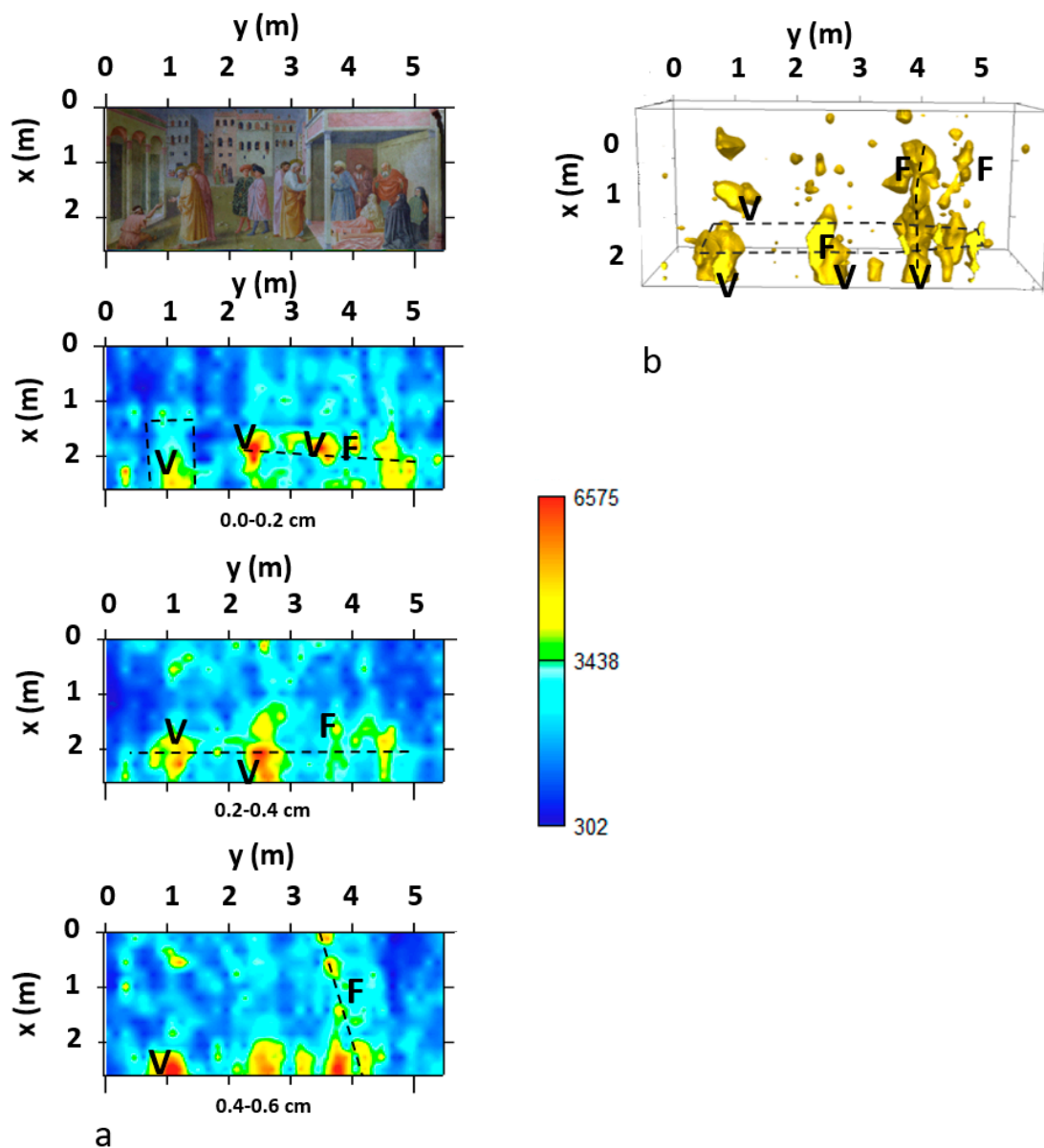
Figure 6. Second floor, right side, large fresco, 900 MHz antenna. (**a**) depth slices 0.0–0.6 m, (**b**) 3D visualization, amplitude isosurfaces. F: fracture; V: empty.

3.2. 2000 MHz Antenna Data Analysis

The 2000 MHz GPR data were processed with: (i) Time–zero correction; (ii) amplitude normalization, consisting of the declipping of saturated (and thus clipped) traces by means of a polynomial interpolation procedure; (iii) manual gain; (iv) Kirchhoff two-dimensional velocity migration [1–3], using the 2D velocity distribution.

In this case, an analysis of the volumetric water content was carried out. The dielectric properties of materials are represented by the relative dielectric permittivity. Its variations are influenced by the presence of water. In fact, the relative dielectric permittivity of water is much higher ($\varepsilon_{r,w}$ = 80) than the relative dielectric permittivity of many minerals that make up the rock matrix ($\varepsilon_{r,g}$ can vary between 3 and 5) and air ($\varepsilon_{r,a}$ = 1) [1,2]. Relative dielectric permittivity, and velocity of propagation of the EM wave, are linked (in the GPR frequency range) by the approximate relationship $v = c/(\varepsilon_r)^{1/2}$, where c is the velocity of propagation of the EM wave in empty space (c = 0.3 m/ns). Thus the knowledge of the variation of the dielectric permittivity, allows the determination of the distribution of the volumetric water content in the materials. Various models can be found in the literature which propose

a relationship between the dielectric permittivity and the properties characterizing the volumetric water content, w. The best known is the empirical equation derived from [8]:

$$w = -5.3 \times 10^{-2} + 2.92 \times 10^{-2} x\, \varepsilon_r - 5.5 \times 10^{-4} x\, \varepsilon_r^2 + 4.3 \times 10^{-6} x\, \varepsilon_r^3.$$

This empirical equation relates the dielectric response, ε_r, of various soil samples (with different degrees of saturation) to their net water content, w. This equation was found to be nearly independent of soil texture, soil bulk density, temperature, and soil salinity [10].

In order to verify the reliability of the Topp equation, an HP impedance analyzer was used to measure the dielectric properties, as a function of the volumetric water content, of some samples of gypsum, plaster, and masonry at high frequencies. The analyzer generates an electrical field in the frequency range of 1 to 2000 MHz. The tests, on a total of 80 samples, revealed that Topp's equation can be applied to this case study, with an error of about 3%.

In order to compare the results obtained with the 2000 MHz antenna, with the results obtained with the 900 MHz antenna, the analysis of the GPR profiles acquired on the second floor is shown in Figure 7. The data allows the investigation of the first 0.4–0.5 m of the wall (with an average velocity of propagation of the electromagnetic wave equal to 0.11 m/ns):

- two horizontal reflected events, linked to the stratification in the first 10 cm of depth; a first layer is identified, with a thickness of about 3.6 cm from the surface, and a second layer with a thickness of about 4.2 cm;
- a series of reflex events, indicated with V, which can probably be interpreted as relating to the presence of small voids; these voids have thicknesses between about 0.3 cm and 0.6 cm.
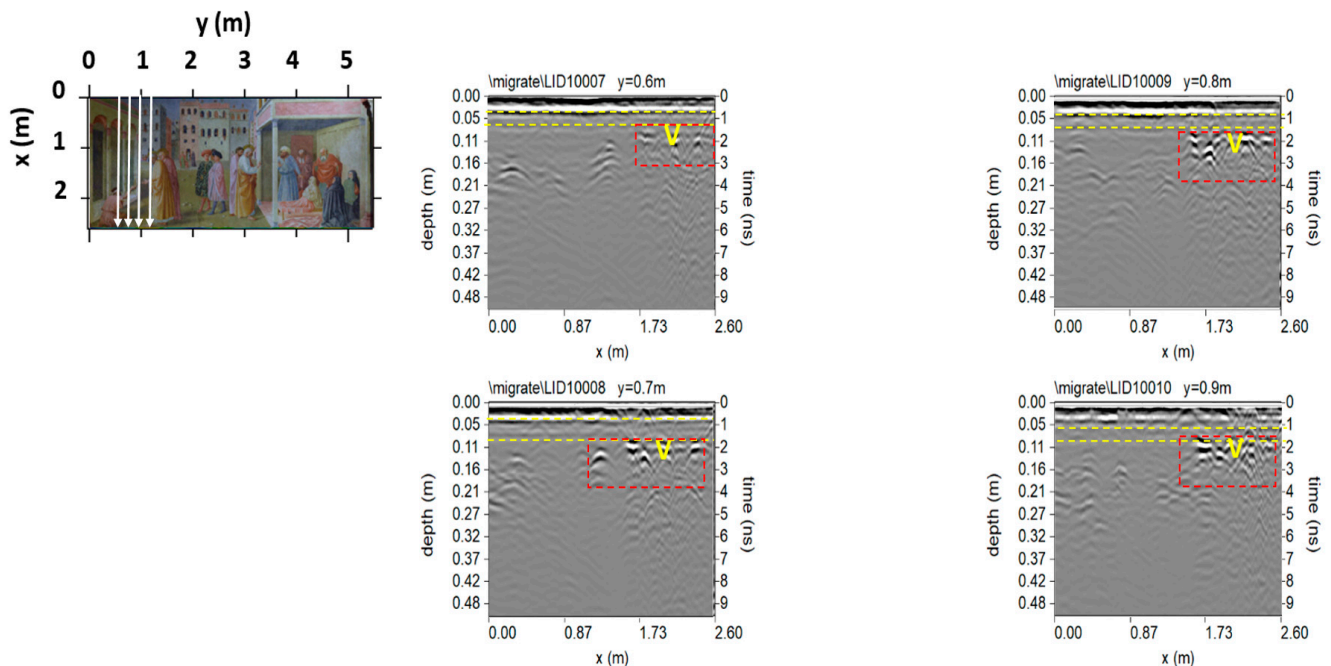
Figure 7. Second floor, right side, large fresco, 2000 MHz antenna: processed radar sections related to profiles 7–10. The dashed yellow lines represent the multi-level stratification (in this case 3). V: probably empty space.

Time slices with a thickness of 0.01 m were made. Figure 8a shows the most superficial slices, from 0.0 to 0.089 m. In these time slices, it is possible to identify the position of the voids (yellow, towards red color) which, also in this case, are most likely linked to detachment conditions. There is also an internal fracture line (F).
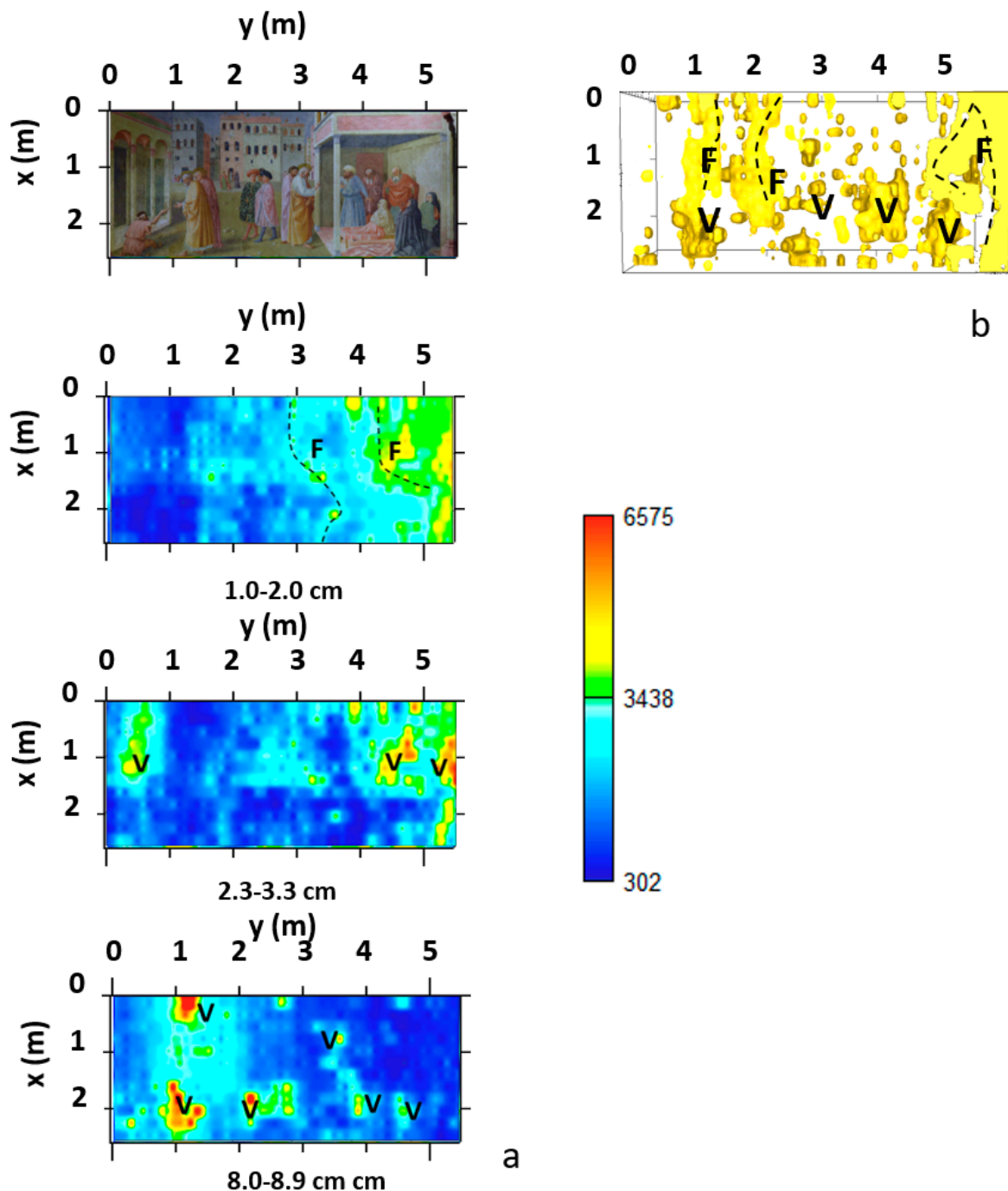
Figure 8. Second floor, right side, large fresco, 2000 MHz antenna: (**a**) depth slices 1.0–2.0 cm, 2.3–3.3 cm, and 8.0–8.9 cm. V: probably empty; F: probable fracture. (**b**) 3D visualization, amplitude isosurfaces. F: fracture; V: empty.

Figure 8b shows a 3D view that allows one to follow the development of F and V anomalies.

The EM wave velocity was determined from the point-source reflections. This method gives rms EM wave velocities to the depth of the point-source reflector. This early application, which uses a point-source reflection from a buried object to determine the average velocity, gives an accurate (qualitative) estimate of the subsoil volumetric water content in the frescoes [1,2]. From the 2D velocity distribution, it is possible to estimate the 2D distribution of the relative dielectric permittivity. By applying the empirical Topp formula, it is possible to obtain an estimate of the 2D distribution of the volumetric water content.

Combining all of the 2D data with the distribution of the volumetric water content, it is possible to build the volumetric water content slices [1,2]

Figure 9 shows the surface slice, which represents the distribution of the volumetric content in water. It is possible to distinguish the zones (H) with the highest values of volumetric content in water (between 4% and 6%).
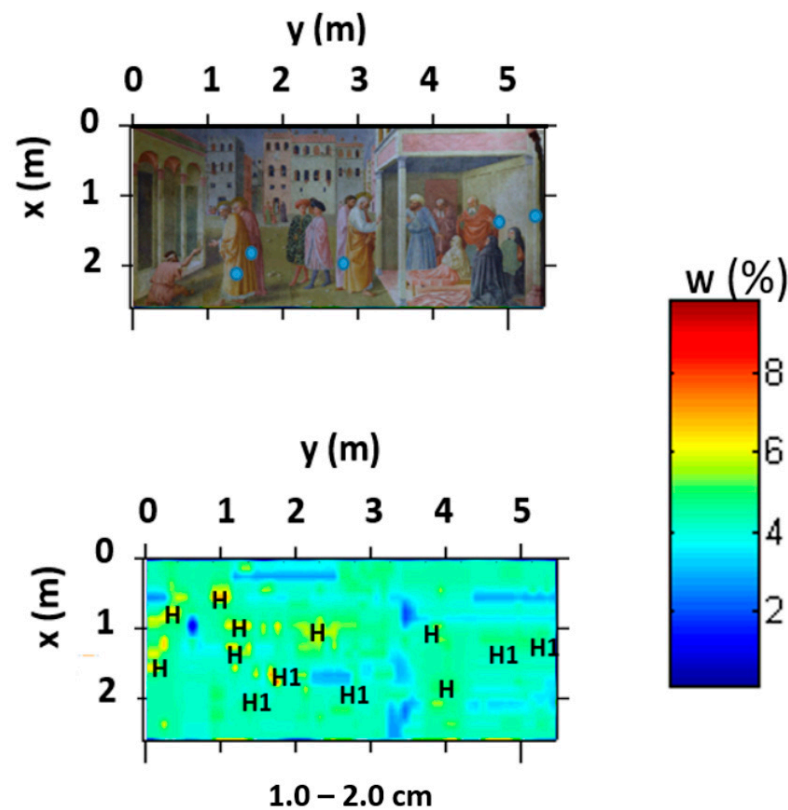
Figure 9. Second floor, right side, large fresco, 2000 MHz antenna: distribution of volumetric content in water; the blue circles indicate the known gypsum injections, which coincide with the areas indicated with H1.

4. Discussion

Integrated data acquisition, using the two antennas with different frequencies, has helped to understand the structures of both the masonry and the frescoes. For the 900 MHz antenna (Figure 4), the data show a high amplitude anomaly, V, in which the electromagnetic wave inverts the polarity. This corresponds to the presence of a high contrast of electromagnetic characteristics, such as those due to the presence of empty spaces [2]. The number of identified voids was about 17. In the anomalies labelled F (fractures), it is possible to see a high amplitude reflection of the electromagnetic waves, but in this case, no polarity change is observed. The number of fractures was about 24.

The data from the 2000 MHz antenna show a higher resolution than the 900 MHz antenna data. In Figure 8 it is possible to see layers of plaster (at least three), and the areas of detachment on the surface, indicated with V, have been identified. The three layers of plaster have thicknesses varying between 0.03 m and 0.04 m. The thickness of the walls is equal to about 0.6 m.

The number of identified superficial voids was about 11. The number of fractures was about 24. The number of points of detachment identified was 22.

It was also possible to better define the more superficial fractures (F) relating to the fresco. In the past years, a restoration intervention had been carried out using gypsum injections. Many intervention points with gypsum injections are not known. For this reason, a study on the volumetric content of water was attempted. Gypsum is a material that

retains humidity and, for this reason, we proceeded to analyze the data first from the point of view of the 3D distribution of the velocity of propagation of the EM waves, and then from the point of view of the distribution of the volumetric content in water (Figure 9), through the estimation of the relative dielectric permittivity. The results could indicate the presence of gypsum injections in the areas (H) with the highest water volumetric content.

Finally, a 3D visualization was created through the amplitude isosurfaces of the data acquired both with the 900 MHz antenna (Figure 10), and with the 2000 MHz antenna (Figure 11). These data were superimposed on the images of the frescoes obtained with photogrammetry, in order to have a precise location of all the anomalies.

Figure 10. 900 MHz antenna: anomalies found (V: void spaces; F: fractures).
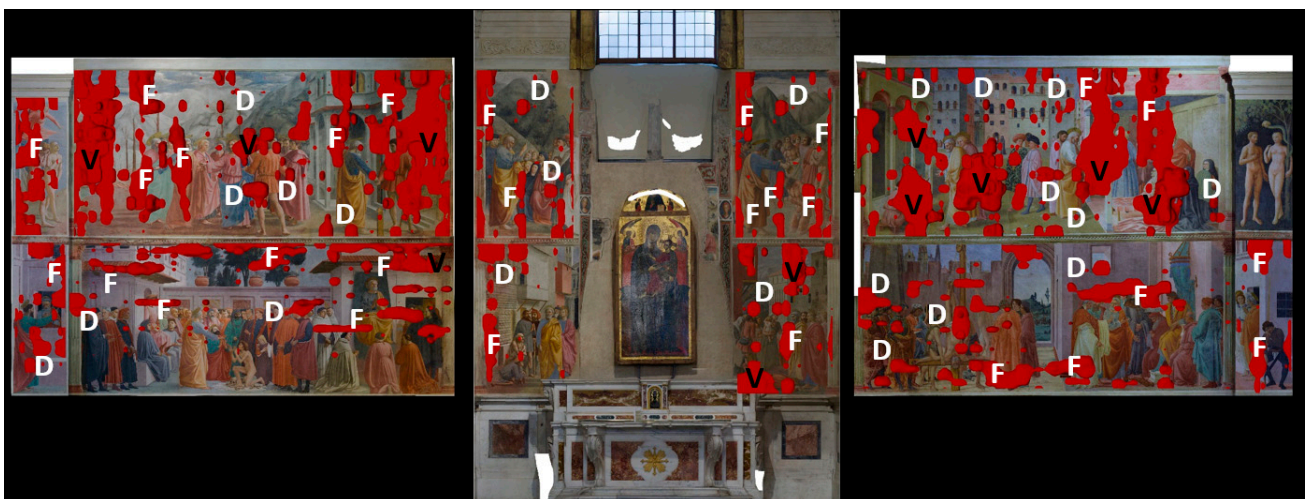
Figure 11. 2000 MHz antenna: anomalies found (D: detachment; F: fractures; V: empty spaces).

Figures 10 and 11 show a worrying situation of degradation in both of the frescoes, with the presence of voids (V), fractures (F), and areas of a detachment of the plaster (D) and of the masonry, with a series of defects (voids and fractures) which can affect stability.

5. Conclusions

Once again the GPR methodology has demonstrated its potential in identifying, with high resolution, some anomalies related to the presence of "defects" both in the masonry and in the frescoes. In particular, the use of the antenna with a central frequency of 2000 MHz has allowed the localization of points of a detachment of the mortars, and

consequently an estimation of the state of adhesion of the mortars, including the frescoes, to the masonry. The stratigraphy of the plaster was also identified. In fact, three layers of plaster, with thicknesses varying between 0.03 m and 0.04 m, were identified. The 3D analysis then made it possible to identify the size and geometry of the detachment areas. The use of the 900 MHz central frequency antenna allowed us to go deeper and to identify the thickness of the walls as being about 0.6 m. In this case, some defects have been identified within the masonry (voids and fractures). The volumetric water content analysis allows the identification of probable small areas of intervention in past years, created through the injection of plaster. Some of these areas coincide with the known injection zones.

References

1. Leucci, G. *Nondestructive Testing for Archaeology and Cultural Heritage: A Practical Guide and New Perspective*; Springer: Berlin/Heidelberg, Germany, 2019; p. 217, ISBN 978-3-030-01898-6.
2. Giannino, F.; Leucci, G. *Electromagnetic Methods in Geophysics: Applications in GeoRadar, FDEM, TDEM, and AEM*; Wiley: Hoboken, NJ, USA, 2021; p. 352, ISBN 978-1-119-77098-5.
3. Conyers, L.B. *Interpreting Ground-Penetrating Radar for Archaeology*; Left Coast Press: Walnut Creek, CA, USA, 2012.
4. Cozzolino, M.; Di Giovanni, E.; Mauriello, P.; Piro, S.; Zamuner, D. *Geophysical Methods for Cultural Heritage Management*; Springer: Berlin/Heidelberg, Germany, 2018; p. 211.
5. Ortega-Ramírez, J.; Bano, M.; Lelo de Larrea-López, L.; Robles-Camacho, J.; Ávi-la-Luna, P.; Villa-Alvarado, L.A. GPR measurements to identify cracks and textural arrangements in the altar Wall of the 16th-century Santa María Huiramangaro Church, Michoacán, Mexico. *Near Surf. Geophys.* **2019**, *17*, 247–261. [CrossRef]
6. De Giorgi, L.; Lazzari, M.; Leucci, G.; Persico, R. Geomorphological and Non-Destructive GPR Survey for the Conservation of Frescos in the Rupestrian Churches of Matera (Basilicata, Southern Italy). *Near Surf. Geophys.* **2020**. [CrossRef]
7. Ortega-Ramirez, J.; Bano, M.; Villa-Alvarado, L.A. GPR for detecting cracks and voids in a historical mural, before restoration, on the altar Wall of a XVII century church. In Proceedings of the 18th International Conference on Ground Penetrating Radar, Golden, CO, USA, 14–19 June 2020; Society of Exploration Geophysicists: Mexico City, Mexico, 2020; pp. 22–25.
8. Topp, G.C.; Davis, J.L.; Annan, A.P. Electromagnetic Determination of Soil Water Content: Measurements in Coaxial Transmission Lines. *Water Resour. Res.* **1980**, *16*, 574–582. [CrossRef]
9. Sandmeier, K.J. *Reflexw 9.0 Manual*, Sandmeier Software; Sandmeier: Karlsruhe, Germany, 2022.
10. Goodman, D. GPR Slice Version 7.0 Manual. 2013. Available online: https://www.gpr-survey.com (accessed on 4 June 2013).